World Academy of Science, Engineering and Technology
International Journal of Mechanical and Materials Engineering
Vol:9, No:8, 2015

A Method to Compute Efficient 3D Helicopters Flight Trajectories Based on a Motion Polymorph-Primitives Algorithm

Konstanca Nikolajevic, Nicolas Belanger, David Duvivier, Rabie Ben Atitallah, Abdelhakim Artiba

***Abstract*—**Finding the optimal 3D path of an aerial vehicle under flight mechanics constraints is a major challenge, especially when the algorithm has to produce real time results in flight. Kinematics models and Pythagorian Hodograph curves have been widely used in mobile robotics to solve this problematic. The level of difficulty is mainly driven by the number of constraints to be saturated at the same time while minimizing the total length of the path. In this paper, we suggest a pragmatic algorithm capable of saturating at the same time most of dimensioning helicopter 3D trajectories' constraints like: curvature, curvature derivative, torsion, torsion derivative, climb angle, climb angle derivative, positions. The trajectories generation algorithm is able to generate versatile complex 3D motion primitives feasible by a helicopter with parameterization of the curvature and the climb angle. An upper "motion primitives' concatenation" algorithm is presented based. In this article we introduce a new way of designing three-dimensional trajectories based on what we call the "Dubins gliding symmetry conjecture". This extremely performing algorithm will be soon integrated to a real-time decisional system dealing with inflight safety issues.

***Keywords*—**Aerial robots, Motion primitives, Robotics.

I. Introduction

SIMULATION relying on dynamics helicopters model raises the problem of computation time. This is particularly right when the problem requires a simultaneous generation of massive set of trajectories (>5000 trajectories over 30 seconds of flight) with a computation loop of 50 milliseconds. In this situation, the use of inflight embedded computation resources becomes critical. This well-known mobile robotics problem has been addressed by a wide variety of research works in the frame of trajectories kinematics model. If the problem of 2D optimal path for a non holonomic robot by the use of motion primitives, with bounded derivative of the curvature, is already addressed by performing algorithms [7], the scientific and technical domain of helicopters 3D flight path generation optimization by kinematics motion primitives is currently rapidly moving [11], [12], [8]. To solve the problem of path of minimal length for aerial vehicle with prescribed initial and final space positions and speed vectors, solutions relying on algorithms for Pythagorian Hodograph curves have been performed [9], [10]. Those solutions are performing to provide valid solutions but they face difficulty to simultaneously control and guaranty saturation of intrinsic trajectory dimensioning constraints like: maximal curvature k_{max}, maximal torsion τ_{max}, maximal climb angle θ_{max}, and their derivatives constraints $(\frac{dk}{ds})_{max}$, $(\frac{d\tau}{ds})_{max}$, $(\frac{d\theta}{ds})_{max}$. Those limits are generally determined by flights tests records and helicopter heavy dynamics models of simulation. In the frame of environment and time bounded helicopters missions, saturating at the same time the flight trajectory above constraints becomes an important challenge. To solve it, 3D flight path generation methods relying on motion primitives have already been performed and provided efficient results [4], [6]. The case of Yasmina Bestaoui works [2] is interesting as it addresses the problematic of transitions between two flight situations by introducing the use of transition curves with linear curvature and torsion, or quadratic torsion. This is of real interest because helicopters manoeuvers to capture an oriented space position under time constraint often require the combination of a climb angle increase and a turn. The established motion is then a helix arc. Before reaching the established motion, flight records and helicopters heavy dynamics simulation models results show that the required transition can be relevantly modeled by the kind of curve with linear curvature and torsion. We address in this contribution a kinematics motion primitives algorithm. This algorithm relies on clothoids, straight segments, spiral arcs and 3D transitions. The main feature of the 3D transitions generated by our algorithm is that their generation relies on an original integration method that can guaranty different forms of 3D transitions with very light parameterization. Moreover, our algorithms authorize very simple laws on curvature κ and climb angle θ parameterized by the curvilinear abscissa s. Therefore, it generates 3D Euler spiral, 3D spiral with quadratic torsion and curves traced on cylinder surfaces. 3D transitions and other described primitives are then aggregated by the means of an algorithm inspired by Dubins curves [5] extended to 3D. We present in the present article a use case with prescribed initial and final: positions, speed vectors, curvature and torsion. We demonstrate the efficiency of the algorithm by comparing lengths of generated path to a 3D Dubins like path with an extremely good ratio (close to 1).

Konstanca Nikolajevic is from the Innovation Department of Airbus Helicopters, Marseille Provence Airport, 13700 Marignane and the University of Valenciennes and Hainaut-Cambresis, Le Mont Houy, 59313 Valenciennes cedex 9, France (e-mail: konstanca.nikolajevic@airbus.com or konstanca.nikolajevic@etu-univ-valenciennes.fr).

Nicolas Belanger is from the Innovation Department of Airbus Helicopters, Marseille Provence Airport, 13700 Marignane, France (e-mail: nicolas.belanger@airbus.com).

David Duvivier, Rabie ben Atitallah and Abdelhakim Artiba are from the LAMIH UMR 8201, University of Valenciennes and Hainaut-Cambresis, Le Mont Houy, 59313 Valenciennes cedex 9, France (e-mail: david.duvivier@univ-valenciennes.fr, Rabie.ben-atitallah,@univ-valenciennes.fr, abdelhakim.artiba@univ-valenciennes.fr).

II. From the Dynamic Model of the Aircraft to a Mathematical Characterization of the Flight

A model, based on mathematical motion primitives and capable of computing accurate flight trajectories, characteristic of the helicopter's dynamics, is of major interest for embedded systems in the sense that it is light to process. However, this model needs characteristic parameters to compute the motion primitives. In order to get these parameters and compute the corresponding motion primitives, a specific method is needed. The method described in this section takes into account the aircraft's dynamics and does not exceed the flight envelope. It has been designed in order to fit the real flight characteristics of a helicopter as it is based on flight recordings produced in simulation. For the purpose of this study, a simplified flight loop of a helicopter has been used to produce the data in a simulation environment. The flight loop used in this section is not representative of a particular helicopter. It has only been used as a tool in order to design and implement the mathematical model and eventually provide a test device. However, if the flight loop happen to change, the resulting model remains valid. The only difference would be in the resulting parameters.

The flight recordings have been produced by acting exclusively on three parameters which permitted to create all the possible combinations of trajectories with graduate solicitation of the aircraft. These three parameters are:

- The true air speed
- The vertical speed
- The roll angle

Hence, three types of trajectories where derived from the simulation:

- Climb trajectory (increase of the vertical speed, true air speed kept constant, no roll angle)
- Lateral trajectory (action on roll angle, no vertical speed, true air speed kept constant)
- Oblique trajectory (combining both variation of vertical speed and roll angle for a constant true air speed)

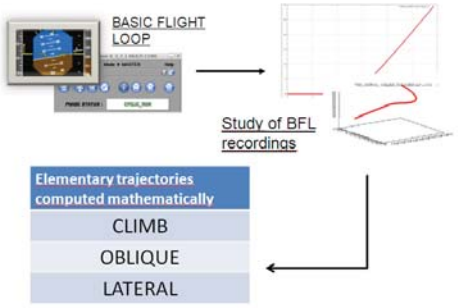

Fig. 1 From the BFL to the mathematically computed trajectories

The lateral and climb trajectories are two-dimensional, as they are contained respectively in horizontal and vertical planes, while the oblique trajectory is three-dimensional.

The data collected in simulation is smoothed using the Bezier curves [3] in order to get the characteristic parameters needed for computing the motion primitives. These parameters are the curvature, the climb angle, and their derivatives. Bezier curves are a convenient choice for this study because a few control points are needed to characterize the simulation recordings. Besides, the most important thing was to characterize the transitions between an initial state with zero curvature, torsion and climb angle to final states where these parameters change simultaneously. Eventually, the resulting curves produced with the Bezier curves smoothing fit very well the simulation data.

III. Trajectories Extracted from the Simulation Model

A. Design of Lateral Trajectories

We define the lateral trajectory as a two-dimensional horizontal path obtained by applying a turn, or a roll angle, to the helicopter. The experiment has been done for different roll angles as shown in Fig. 2.

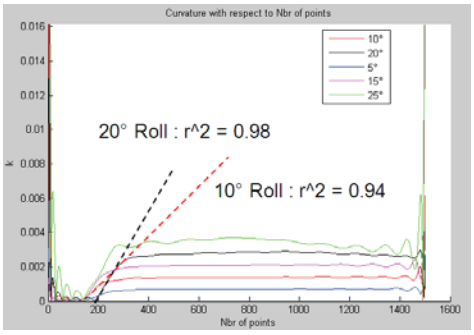

Fig. 2 Curvature profiles obtained from simulation data, with Bezier curves smoothing - results computed for different roll angles

From the simulation recordings, parameters have been extracted such as the maximum curvature κ_{max} and the maximum derivative of the curvature $d\kappa_{max}$. Indeed, the simulation data for such trajectories have permitted to establish a common profile for the curvature distributions. It is noted in Fig. 2, that the curvature changes linearly with the arc length of the curve before reaching a maximum value and remaining constant. Besides, we do not take the maximum values observed in simulation for those parameters. A security margin is kept in order to avoid exceeding the flight envelope and therefore the actual capabilities of the helicopter. Hence the first portion of the lateral trajectory, until S_1 is reached, is a clothoid followed by a circle arc with constant curvature κ_{max} and radius $R = \frac{1}{\kappa_{max}}$; where

$$S_1 = \frac{\kappa_{max} - \kappa_0}{d\kappa_{max}}$$

and S_{tot} depends on the speed and flight time of the aircraft.

Fig. 4 displays a result comparing the trajectory obtained in simulation with the computed trajectory for 30 seconds of flight at a speed of 70 knots. The computed path is very close to the simulation data.

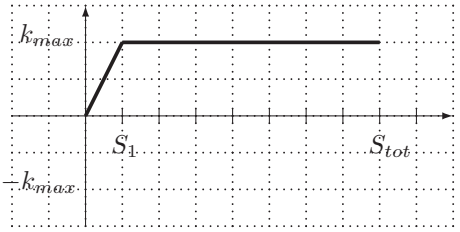

Fig. 3 Diagram of the curvature distribution for a lateral trajectory

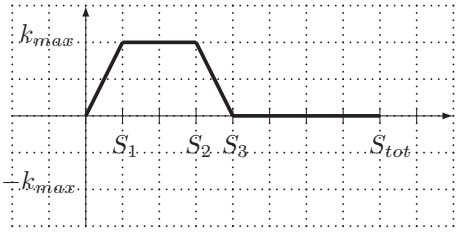

Fig. 6 Diagram of the curvature distribution for a climb trajectory

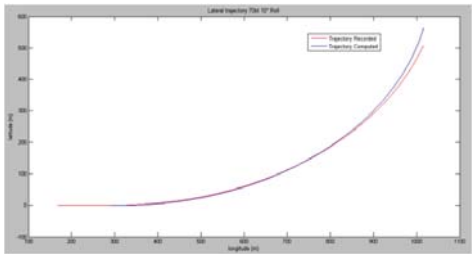

Fig. 4 Results for a lateral trajectory during 30s of flight - simulation (red) and computed trajectory (blue)

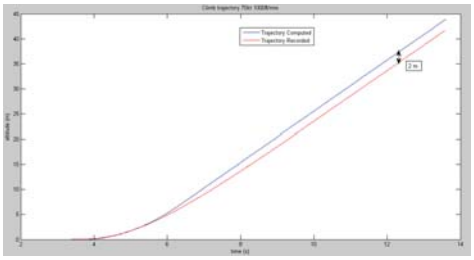

Fig. 7 Results for a climb trajectory on 12 seconds - simulation (red) and computed trajectory (blue)

B. Design of Climb Trajectories

We define a climb trajectory as a two-dimensional vertical path obtained by applying a vertical speed to the helicopter. In the same way as for lateral trajectories, the experiment has been done for different vertical speeds. An example is displayed in Fig. 5.

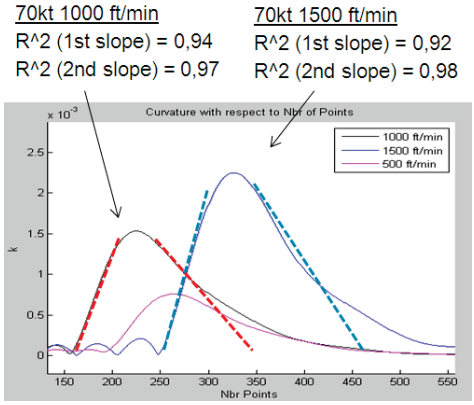

Fig. 5 Curvature profiles obtained from simulation data, with Bezier curves smoothing for climb trajectories at different vertical speeds

Four distinct parts have been identified in the climb trajectories, suggesting four different motion primitives, which are two clothoids (for the linear evolution of the curvature), a circle arch between the clothoids and a straight line with zero curvature at the end (Fig. 6). Here again, we do not take the maximum values found for κ_{max} and the $d\kappa$ slopes. S_1 and S_{tot} are found the same way than for the lateral trajectory. In simulation, we have S_3 as it corresponds to the final climb angle of the climb trajectory, which permits to deduce S_2.

Results for a climb trajectory are displayed in Fig. 7.

When the straight line is captured the final angle of climb is reached. The computed trajectory is compliant with the capabilities of the helicopter. It does not exceed the actual climb performances but remains very close to the simulation for a given vertical speed.

C. Design of Oblique Trajectories - Focus on the Three-Dimensional Spiral Transition

The oblique trajectory is obtained in simulation by both increasing the vertical speed and applying a turn, *i.e.* a roll angle, to the helicopter. The simulation results were performed with different vertical speeds and roll angles. In order to extract the characteristic parameters of this trajectory and capture its different states and stages with the intention of reproducing it mathematically, only initial conditions have been imposed with zero torsion and zero curvature. From there on, we have an open loop trajectory generation system allowing all possible observations.

According to the fundamental theorem of (the local theory of) space curves [1], *"in differential geometry, every regular curve in three-dimensional space, with non-zero curvature, has its shape (and size) completely determined by its curvature and torsion. A curve can be described, and thereby defined, by a pair of scalar fields: curvature κ and torsion τ, both of which depend on some parameter which parametrizes the curve but which can ideally be the arc length of the curve. From just the curvature and torsion, the vector fields for the tangent, normal, and binormal vectors can be derived using the Frenet-Serret formulas. The integration of the tangent field (done numerically or analytically) yields the curve"*.

Since the curves we are dealing with are regular and C^{∞}, knowing their torsion and curvature for all points ensures their unicity. However, even if the Bezier curves smoothing works perfectly fine for finding the curvature distribution along the oblique trajectory taken from the simulation recordings, this method reveals some oscillations with the torsion which makes it difficult to identify formally the maximum value of the derivative of the torsion $d\tau_{max}$. Despite these considerations the method enables to find the maximum value of the torsion

τ_{max} because the distribution stabilizes after the oscillations. The discrete derivation directly from the simulation recordings has also been tested but this method does not give satisfying results either. This is why a specific method for the design of the oblique trajectory is required here. We note that the Bezier curves smoothing method gives a linear evolution of the curvature when both the vertical speed is increased and a turn is applied to the aircraft. An example is displayed in Fig. 8.

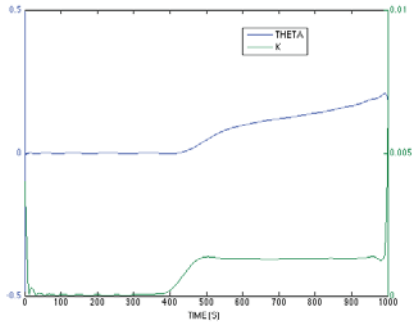

Fig. 8 Distribution of the curvature κ for oblique trajectory with 1000 ft/min vertical speed and 20 degrees roll angle

Actually, it has been observed in simulation at some point that the helicopter captures a helicoidal climb. At this stage, the curvature is maximal and the torsion of the trajectory measured in simulation is also saturated, therefore we have κ_{max}, τ_{max} and θ_{max}. Moreover, we are able to objectivize the derivative of the curvature $d\kappa_{max}$. Regarding these considerations wa are able to suggest a relevant helicoidal trajectory given the capabilities of the helicopter with τ_{max} and κ_{max}. The parametric equations of a circular helix are:

$$\begin{cases} x(t) = a\cos(t) \\ y(t) = \epsilon a \sin(t) \quad \text{with} \quad \epsilon = \pm 1 \\ z(t) = bt \end{cases}$$

Parameters a and b are derived from the radius of curvature $R_c = \frac{1}{\kappa} = \frac{c^2}{a}$ and the radius of torsion $R_t = \frac{1}{\tau} = \epsilon\frac{c^2}{b}$. However, what happens before the helix has to be computed differently. At this stage, we can compute the final torsion as follows:

$$\tau_{max} = \tan(\theta_{max})\kappa_{max}$$

, where κ_{max} is the maximum curvature and θ_{max} is the final angle of climb:

$$\theta_{max} = \arctan(\frac{P_z}{R}) = \arctan(P_z\kappa_{max})$$

, where P is the first point of the helix spiral as shown in Fig. 11 and $R = \frac{1}{\kappa_{max}}$ is the radius of the cylinder ($\mathscr{C}$). Therefore, observations show that the oblique trajectory is composed of a helicoidal path preceded by a three-dimensional spiral transition, which has to be computed taking into account the curvature and climb angle at ($\mathscr{P}$). Moreover, the curvature and remaining climb angle distributions, during the 3D spiral transition, respectively increase and decrease linearly as shown in Fig. 9.

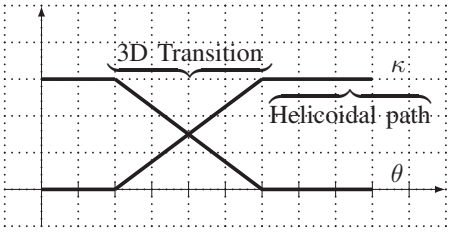

Fig. 9 Diagram of curvature k and remaining climb angle θ distributions for the three-dimensional spiral transition

We suggest a simple integration method for the 3D spiral transition based on elementary helix spirals in the sense that each elementary spirals would have:

- a constant elementary curvature κ_i
- a constant elementary climb angle θ_i
- a constant elementary torsion τ_i

as shown in Figs. 10 and 11. Moreover using a helix spiral is the easier way to approximate a skew curve. Besides, the elements are computed with the maximum derivative of the curvature $d\kappa_{max}$, hence sustaining the optimality of the length s of the 3D spiral transition towards the helix. At the end of every infinitesimal helix spiral, a new center of the helix is computed as well as updated helix parameters a_i and b_i in order to process the next spiral portion as shown in Fig. 10. This process is repeated until the final curvature κ_{max}, the final climb angle θ_{max} and therefore the final torsion τ_{max} are reached.

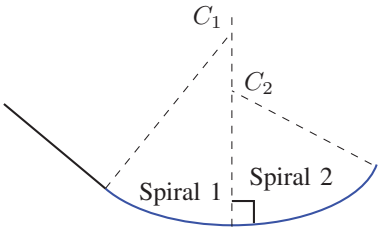

Fig. 10 Framework of the design of the 3D spiral transition as a series of infinitesimal spirals (blue), top view

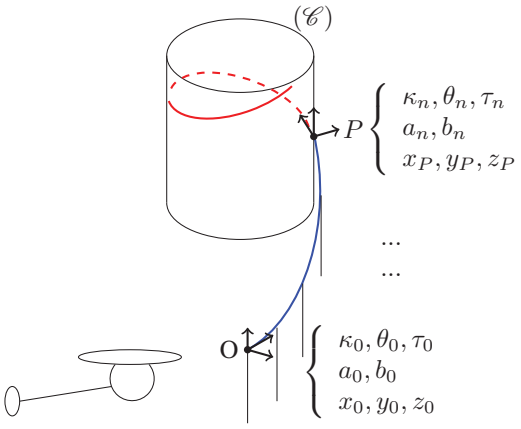

Fig. 11 Framework of the oblique trajectory with the three-dimensional spiral transition (blue) connected to the helicoidal path (red) at point P

Besides, by acting only on the distributions of the curvature and climb angle along this spiral transition we have:

$$\begin{cases} \kappa(s) = \alpha s \\ \theta(s) = \beta s \end{cases} \quad (1)$$

where κ is the curvature and θ is the remaining climb angle. They are both expressed as a function of s, the curvi linear abscissa.

The torsion is defined as $\tau = \kappa \tan(\theta)$, using (1) we have:

$$\Leftrightarrow \tau = \alpha s \tan(\beta s)$$

$$\Rightarrow \frac{d\tau}{ds} = \alpha \tan(\beta s) + \frac{\alpha\beta s}{\cos(\beta s)^2}$$

$$\approx \alpha\beta s + \alpha\beta s \frac{1}{(1 - \frac{(\beta s)^2}{2!})^2}$$

$$\approx \alpha\beta s + \alpha\beta s \frac{1}{1 + 2\frac{-(\beta s)^2}{2!}}$$

$$\approx \alpha\beta s + \alpha\beta s(1 + (\beta s)^2)$$

Neglecting the higher terms,

$$\frac{d\tau}{ds} = 2\alpha\beta s \Rightarrow \tau(s) = \alpha\beta s^2 \quad (2)$$

The torsion is parabolic along the 3D spiral transition with κ and θ evolving linearly from initial conditions $\kappa = 0$ and $\theta = 0$ to κ_{max} and θ_{max}.

In the case when the 3D spiral transition is maintained at maximum curvature κ_{max}, *i.e.* the curve is evolving on a cylinder with radius $R = \frac{1}{\kappa_{max}}$, the previous discussion becomes slightly different.

$$\begin{cases} \kappa = \alpha \\ \theta(s) = \beta s \end{cases} \quad (3)$$

$$\tau(s) = \kappa \frac{b}{a}$$

$$\tau(s) = \kappa \tan(\beta s) \approx k\beta s$$

The torsion is linear.

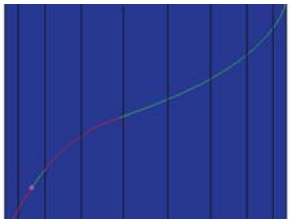

Fig. 12 Change of torsion on a cylinder for the 3D spiral transition (red curve) with curvature constant along the transition and equal to k_{max}

Finally, there is a third case to be considered, when the 3D spiral transition is maintained at constant climb angle and varying curvature. Typically to make a transition from a helix spiral at maximum curvature κ_{max} to a straight line with zero curvature $\kappa = 0$.

$$\begin{cases} \kappa = \alpha s \\ \theta(s) = \beta \end{cases} \quad (4)$$

$$\tau(s) = \kappa \frac{b}{a}$$

$$\tau(s) = \kappa s \tan(\beta) \approx k\beta s$$

The torsion is linear.

As a conclusion, the three-dimensional spiral transition described in this section can take different shapes by only acting on its initial and final inputs which are mainly the curvature κ and the angle of climb θ.

- If $\theta =$ constant, then we obtain a three-dimensional Euler spiral
- If $(\theta_0, \kappa_0) = (0, 0)$ and $(\theta_{final}, \kappa_{final}) = (\theta_{max}, \kappa_{max})$, then we obtain the 3D spiral transition with a quadratic torsion (2).
- If $\kappa =$ constant and θ is linear as derived from (4) then we can obtain a curve plotted on a cylinder surface, which is very convenient for decreasing the torsion of a path when the curvature must remain constant (Fig. 12).

IV. Computing an Efficient Three-Dimensional Trajectory between Two Positions for a Helicopter Flight

Connecting two positions, with different orientations, in the three-dimensional space is not an easy matter. Actually finding an optimal path is quite challenging in the sense that the classical three-dimensional (3D) mathematical curves do not always fit the performances of the aircraft. In the two-dimensional space, the optimal path between two vectors is the C-L-C Dubins path. In 3D, this solution is not valid any more but the idea of an optimal path based on the same concept is not absurd providing that the straight line between the connection points on the initial and final circles has an additional varying vertical component. However, the continuity of the curvature along this path (in a 3D or 2D configuration) is not sustained and if the path had to be flown by a helicopter with passengers on board, it would be very difficult to follow it properly. This is why making smooth transitions based on the helicopter's actual performances between the motion primitives composing the path is of major importance. This section is addressing the design of a feasible 3D trajectory between two possible flight headings, fitting the helicopter's flight model without exceeding the flight envelope. Besides the design is based on a framework composed of a series of 2D and 3D mathematical motion primitives developed in the previous section. First of all, the trajectory is computed for random directions contained in non parallel horizontal planes. In a second step, the trajectory is adapted to form a transition between two way points with their respective headings between two different flight levels. Eventually, the 3D trajectory is compared to what we call a 3D Dubins-like path for comparison.

A. Positioning of the Problem

There are two possible configurations when connecting two vectors $\overrightarrow{AA'}$ and $\overrightarrow{BB'}$ in the three-dimensional space. Either these two vectors are both contained in two parallel plane surfaces, *i.e.* their vertical component is constant $z_A = z_{A'}$,

$z_B = z_{B'}$ and $z_A = \alpha z_B$, where α is constant, but not necessary $z_A = z_{A'} = z_B = z_{B'}$ because we want to join two different heights in this study; or, they are randomly oriented, *i.e.* $z_A \neq z_{A'}$ and $z_B \neq z_{B'}$. In order to take the most general case, we choose to mix these two configurations as shown in Fig. 13 for the definition of the initial and final conditions of the problem in Fig. 14. Thus $z_A \neq z_{A'}$ and $z_B = z_{B'}$.

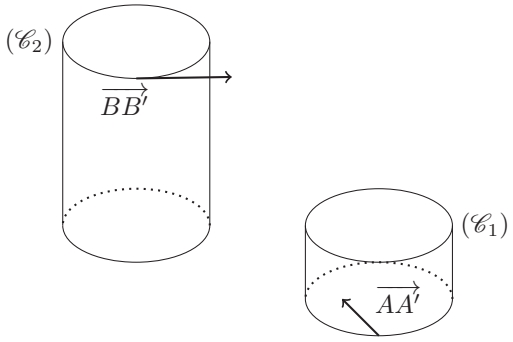

Fig. 13 Three-dimensional view of the problem

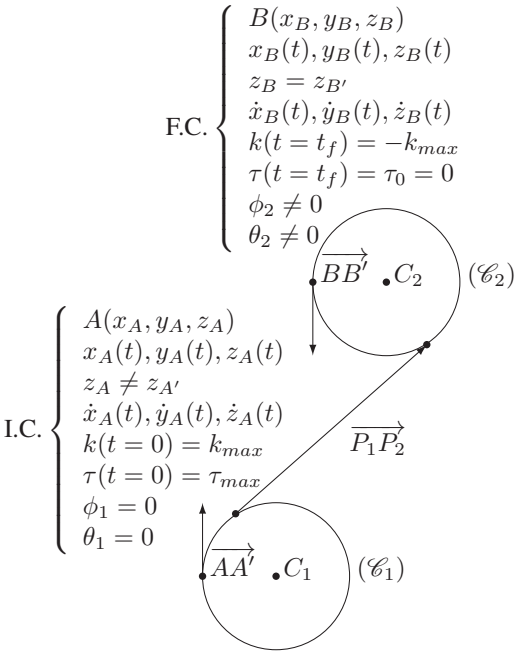

Fig. 14 Two dimensional top view of the problem

The initial conditions (I.C.) are reported in A and the final conditions (F.C.) are reported in B (Fig. 14). C_1 and C_2 are the centers of cylinders $(\mathscr{C}_1)$ and $(\mathscr{C}_2)$. The design of the 3D trajectory is based on the idea of the two-dimensional Dubins path. However, we are reasoning on three-dimensional geometric objects instead. We note that the 3D trajectory, will include a change of direction (curvature going from $k(t = 0) = k_{max}$ to $k(t = t_f) = -k_{max}$) in order to fit the final condition requirements. Hence, two concerns are addressed here:

- The first concern is finding a way to connect cylinder $(\mathscr{C}_1)$ to cylinder $(\mathscr{C}_2)$ taking into account the curvature constraints.
- The second concern is making the path between the cylinders coincide vertically.

In Fig. 14, $\overrightarrow{P_1P_2}$ is the vector between points P_1 on $(\mathscr{C}_1)$ and P_2 on $(\mathscr{C}_2)$. $\overrightarrow{P_1P_2}$ is tangent to both cylinders. In a two-dimensional Dubins path planning, the line directed by vector $\overrightarrow{P_1P_2}$ would be one way of connecting circle arcs between A and P_1 and between P_2 and B. Since we are in 3D, and in a concern of designing the shortest 3D trajectory between A and B we have helix spirals, combining both a climb and a turn, instead of circle arcs between points A and P_1 and between P_2 and B.

However, as the 3D trajectory would obviously need a change of direction at some point because the curvature at I.C. is the opposite of the curvature at F.C., the three-dimensional spiral transitions developed in section III-C will be used to ensure the sustainability of the curvature along the 3D path. It is assumed that the transitions have a fixed length every time they are used so the design of the final trajectory can be focused on finding the shortest length for the other 3D motion primitives. The 3D spiral transition is used with the purpose of making the link between the motion primitives, without exceeding its own capacities (derivative of the curvature dk and maximum climb angle θ).

B. Finding the Plane Containing the Straight Line between S_2 and S_3 with the Dubins Gliding Symmetry Conjecture

The Dubins gliding symmetry conjecture is applicable for a Dubins CLC path type when the initial and final positions have opposite curvature values. The conjecture relies on computing a point M, which stands for the middle of the $[P_1, P_2]$ segment, where P_1 and P_2 are respectively the tangent points of line (P_1P_2) to circles $(\mathscr{C}_1)$ and $(\mathscr{C}_2)$ as shown in Fig. 15. For the purpose of this study and in a concern of symmetry compliance, it is assumed that the 3D spiral transition size is constant along the 3D trajectory and computed with saturated constraints in curvature and torsion until $(\mathscr{C}_2)$ is reached.

The Dubins gliding symmetry conjecture is used in Fig. 14 to find a matching direction between the cylinders. The plane containing the vector $\overrightarrow{P_1P_2}$ is tangent to $(\mathscr{C}_1)$ and $(\mathscr{C}_2)$ and could contain a straight line going from the initial cylinder to the final one. However, instead of having a plane making a direct link between $(\mathscr{C}_1)$ and $(\mathscr{C}_2)$ we need to find here a plane containing the final direction of $Transtion1$ and the initial direction of $Transition2$ (Fig. 17). To put in a nutshell, we have two 3D spiral transitions, one going up from $(\mathscr{C}_1)$ and another going down from $(\mathscr{C}_2)$, and they need to be aligned so their final points could be connected by a straight line in order to establish a link between $(\mathscr{C}_1)$ and $(\mathscr{C}_2)$. Since the spiral transitions have the same lengths, this problem is reduced to finding the size of the initial helix spiral on $(\mathscr{C}_1)$, which is equivalent to finding S_1 (Fig. 17) when the final direction vector of $Transition1$, $\overrightarrow{d_{T_1}}$ and the final transition vector of $Transition2$, $\overrightarrow{d_{T_2}}$ are colinear (Fig. 15):

Let $\overrightarrow{d_{T_1}}$ be defined as $\overrightarrow{d_{T_1}} \begin{cases} d_{T_{1,i}} \\ d_{T_{1,j}} \end{cases}$, and $\overrightarrow{d_{T_1}}$ be defined as $\overrightarrow{d_{T_2}} \begin{cases} d_{T_{2,i}} \\ d_{T_{2,j}} \end{cases}$, $\overrightarrow{d_{T_1}}$ and $\overrightarrow{d_{T_2}}$ colinear $\Leftrightarrow$ $d_{T_{1,j}} d_{T_{2,i}} = d_{T_{2,i}} d_{T_{1,j}}$.

Since the climb angle is already given by the climb rate

of the spiral transition from $(\mathscr{C}_1)$, there is no need to take into account the vertical component of $\overrightarrow{d_{T_1}}$ and $\overrightarrow{d_{T_2}}$. However, we do not know from what point the 3D spiral is computed on $(\mathscr{C}_2)$. The Dubins gliding symmetry conjecture solves this problem by taking into consideration a symmetrical construction of the path between the cylinders by giving a special importance to the middle point M (Fig. 15). Therefore, the algorithm for finding a common direction to $\overrightarrow{d_{T_1}}$ and $\overrightarrow{d_{T_2}}$ is simple. The principle is finding a final vector $\overrightarrow{d_{T_1}}$ colinear to $\overrightarrow{P'M}$ and increase S_1 until this condition. A result is presented in Fig. 16.

$$\Leftrightarrow d_{T_{1,i}} y_{\overrightarrow{P'M}} - d_{T_{1,j}} x_{\overrightarrow{P'M}} = 0$$

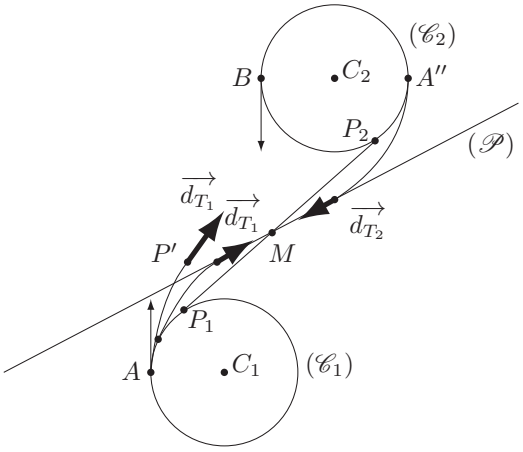

Fig. 15 Finding plane $(\mathscr{P})$, the link between $(\mathscr{C}_1)$ and $(\mathscr{C}_2)$ with $AP_1 < BP_2$ - top view

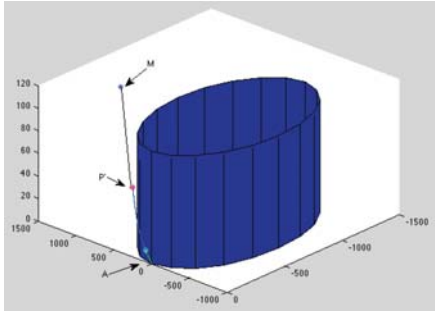

Fig. 16 Cylinder $(\mathscr{C}_1)$ with the helix spiral and the 3D transition spiral connecting M

The second concern is to make both direction vectors $\overrightarrow{d_{T_1}}$ and $\overrightarrow{d_{T_2}}$ coincide vertically. This is ensured by the climb rate at the end of $Transition1$. By point reflection through M and keeping the same climb coefficient we have the altitude of A'' on $(\mathscr{C}_2)$.

The final distribution of the curvature along the 3D trajectory designed with the Dubins gliding symmetry conjecture is given by Fig. 17. S_1 is obtained by a scan between A and P_1 on $(\mathscr{C}_1)$. When S_1 is reached (Fig. 16) the curvature decreases to zero until S_2 in order to meet the common plane going through M (Fig. 15). By symmetry, the path from M to A'' on $(\mathscr{C}_2)$ is completed until S_4 and the

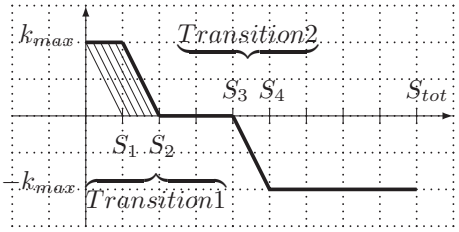

Fig. 17 Framework of the curvature along the three-dimensional trajectory between A and B given by the thick black polygonal chain

final condition on the curvature as specified initially (Fig. 14) is achieved.

Once $(\mathscr{C}_2)$ is reached with a given climb angle, it may happen that this climb angle is too big to achieve the F.C. at B, and exceeds the final altitude. Thus, the torsion of the 3D helix spiral on $(\mathscr{C}_2)$ must be reduced and the remaining series of motion primitives contained between S_4 and S_{tot} should have their torsion and hence their length adapted to satisfy the final requirements.

C. Finding the Final Torsion Distribution on $(\mathscr{C}_2)$

Now that the cylinders are connected by a feasible path, the last concern consists into finding the final torsion distribution on $(\mathscr{C}_2)$. Indeed, from the beginning we are looking for the most efficient path between the initial point A and final point B. This conveys the idea of a maximum climb rate feasible by the aircraft from the initial state. However, if this climb rate is maintained, the trajectory might go too far and never reach B. This is why finding an adapted torsion distribution on $(\mathscr{C}_2)$ ensures a smooth path from A'' to B (cf Fig. 15). The path arrives with maximum torsion at A'' and needs to reach B with zero torsion according to I.C. and F.C. in Fig. 14. Thus, we need at least two 3D spiral transitions and one helix spiral to reach the point B. The first 3D spiral transition would make the path go from τ_{max} to $\tau_{new(\mathscr{C}_2)}$ (the new torsion), keeping the curvature κ_{max}. The last one would connect the end of the helix spiral at $\tau_{new(\mathscr{C}_2)}$ to point B making the torsion decrease to zero and still with κ_{max} everywhere. Hence the remaining angle to reach from A'' to B is defined as:

$$\theta_{remaining} = \Delta\theta_1 + \Delta\theta_2 + \Delta\theta_3$$

where $\Delta\theta_1 = \theta_r - \theta_{max}$ is the angle difference for the first spiral transition on $(\mathscr{C}_2)$; $\Delta\theta_2 = 0 - \theta_r$ is the angle difference for the second spiral transition (final transition to arrive at point B with zero torsion) and $\Delta\theta_3$ is the angle difference for the helix spiral between Transition 2 and Transition 3.

Finding the final torsion to get a smooth path from A'' to B results into finding θ_r, which stands for the optimal climb angle given that the torsion should remain lower than the maximum torsion on $(\mathscr{C}_2)$. Hence $\tau_{new(\mathscr{C}_2)} = k_{max}\tan(\theta_r)$ (Algorithm 1).

D. Connecting Two Different Flight Levels with a Three-Dimensional Trajectory

The previous discussion has addressed the design of a three-dimensional trajectory based on a series of motion

primitives. The purpose was to connect two vectors whose directions were chosen randomly in order to have the most general configuration to deal with. However, in most cases, the helicopter would have to fly from a flight level to another, *i.e.* from a horizontal plane with a given altitude to another horizontal plane with higher or lower altitude. This means that the helicopter would need a three-dimensional trajectory connecting two vectors contained in parallel planes.The only difference with the previous problem described in IV-A is that the initial vector $\overrightarrow{AA'}$ (Fig. 14) is contained in a plane surface and therefore the three-dimensional trajectory is composed of an additional 3D spiral transition going from zero curvature $\kappa_0 = 0$ and zero torsion $\tau_0 = 0$ to point A with κ_{max} and τ_{max}. Therefore, the method to compute the 3D trajectory is identical and the Dubins gliding symmetry conjecture starts at point A, where the curvature is κ_{max} and the torsion is τ_{max}.

The algorithm 1 sums up the method used to compute the three-dimensional trajectory between A and B. L_{h_1} and L_{h_2} are respectively the lengths of the first helix spiral on the cylinder ($\mathscr{C}_1$) and the second helix spiral on the cylinder ($\mathscr{C}_2$). $\theta_{remaining}$ is the angle between points A'' and B.

Algorithm 1 3D trajectory from A to B

1) COMPUTE Dubins circles and cylinders

2) FIND Tangent plane ($\mathscr{P}$) with the Dubins gliding symmetry conjecture
Compute M = middle of $[P_1, P_2]$
INITIALIZE $L_{h_1} = 0$
if $\overrightarrow{P'M}$ and $\overrightarrow{d_{T_1}}$ not colinear **then**
  Increment L_{h_1}
end if
return Tangent plane ($\mathscr{P}$) and Trajectory Trj to M

3) Point reflection / M of Trj taking into account the climb angle in order to get to ($\mathscr{C}_2$)

4) Adapt torsion on ($\mathscr{C}_2$) in order to reach B
COMPUTE $\theta_{remaining}$
COMPUTE θ_{max}
for $\theta_r = \theta_{remaining}/3, ..., \theta_{max}$ **do**
  COMPUTE 3D spiral transition from τ_{max} to τ_r
  Compute L_{h_2}
  Compute helix spiral for L_{h_2}
  COMPUTE 3D spiral transition $T_{\tau_r \to \tau_{final}}$ from τ_r to $\tau_{final} = 0$
  if final point of $T_{\tau_r \to \tau_{final}}$ = B **then**
    Break
  end if
end for
return θ_r

There are two problems to take into account: a two-dimensional problem where it is important to find the right direction to connect points A and B as a top view; and a three-dimensional problem where the vertical directions have to match too. Computing the Dubins circles permits to find the shortest path to connect two oriented points in the two-dimensional space. Therefore, it gives a frame for the design of the 3D trajectory between A and B using the Dubins gliding symmetry conjecture. Eventually, the 3D trajectory is connected to the final point B by adapting the torsion distribution on cylinder ($\mathscr{C}_2$). Indeed, in an attempt of having an efficient 3D trajectory we keep the constraints of curvature, torsion and climb angle saturated until ($\mathscr{C}_2$) is reached. In this paper, it is assumed that the altitude of point B is not exceeded when ($\mathscr{C}_2$) is reached. However, the climb rate should be adapted thereafter by computing a new climb rate θ_r which takes into account both, the final condition in B where $\theta = 0$, and the variation of θ due to the transitions and the helix spiral used to make the link. This last problem is decomposed in three parts:

- go from θ_{max} to θ_r
- keep the climb rate θ_r constant on the helix spiral
- go from θ_r to $\theta = 0$ in order to satisfy the final condition and therefore reach a horizontal plane in B

E. Comparison with the "3D Dubins Path"

In an attempt of trying to compute an efficient 3D trajectory the results have been compared to a 3D Dubins-like path computed for a constant climb rate from A to B. Just as the path computed using the Dubins gliding symmetry conjecture, it is composed of two helix spirals connected by a straight line between the points P_1 and P_2 (Fig. 15). This path is not constant in curvature and absolutely not feasible by a helicopter. However, it is the shortest Dubins-like 3D path we could obtain for comparison with the Dubins gliding symmetry conjecture results. Using the Dubins gliding symmetry conjecture we have the length d. We decide to withdraw the length of the straight line SL for comparison which gives the following ratio

$$\frac{D - SL}{d - SL} = 0.9955$$

which makes the actual 3D path very close in terms of length to the shortest 3D path we could obtain here. A result is displayed in Fig. 18.

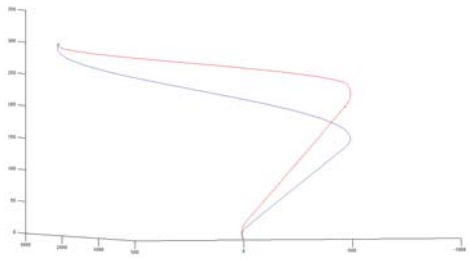

Fig. 18 3D Trajectory computed in red with the Dubins gliding symmetry conjecture compliant in curvature and torsion and the "Dubins-like 3D trajectory" in blue, not feasible by a helicopter

V. Conclusion and Further Works

This article addressed the complex problem of 3D minimum length paths for a helicopter between two arbitrary oriented

space positions. Regarding flight manoeuvres performed by test pilots recorded during simulation sessions, we identified a set of motion primitives necessary and sufficient to build up 3D shortest paths compliant with helicopters flight operational constraints. Different skew curves have been identified and modelled thanks to Airbus Helicopters flight simulation data observations like: circular spiral arc, 3D Euler spiral, spiral with quadratic torsion, curve plotted on cylinder with linear climb angle and linear curvature. On top of those motion primitives, we added classical primitives used in aerial robotics problems: clothoids (in horizontal and vertical plans), circular arcs, straight segments. Objectivizing on the basis of simulation data (approximated by Beziers curves), the limits of: curvature, derivative of the curvature, climb angle, derivative of the climb angle and finally torsion, we approached very closely the helicopter's behavior in a kinematics way. To solve the complex problem of finding 3D path of minimal length for two arbitrary oriented spec positions under helicopters flight mechanics constraints, we built a new kind of algorithm. This algorithm integrates the innovative concept that we introduce as the 'Dubins gliding symmetry conjecture'. This principle allows the optimal and formal determination of a vertical plane that two 3D transitions shall meet to further grab two distant spiral arcs. The exact tangents points (positions and climb angles) in the vertical plane are also determined using this principle. The introduced principle allows minimization of the 3D path as it is shown by the calculation of a 3D minimal length with discontinuity on curvature and torsion. On top of that, the algorithm is of real interest in the way it manages very simply the choice, the calculation and the distribution of the motion primitives. The low complexity of the algorithms makes very optimistic its use for massive parallel generation of combined primitives in the perspective of an upper system using this trajectory generation module and requiring real time performances. To improve the algorithm, a human dimension could be taken into account. Indeed, if the generated trajectories are feasible according to the helicopters flight mechanics constraints, it has still to be proven that in certain cases the pilot would effectively chose it. In order to validate this work, a simulation campaign with flight tests pilots in the loop should be organized, and the algorithm will be adapted accordingly to the pilot's behaviors facing complex flight situations.

REFERENCES

[1] T. F. Banchoff and S. T. Lovett, *Differential geometry of curves and surfaces*. CRC Press, 2010.

[2] Y. Bestaoui, "General representation of 3d curves for an unmanned aerial vehicle using the frenet-serret frame," *AIAA*, 2007.

[3] P. Bezier, "Essais de definition numeriques des courbes et surfaces non mathematiques," *Systeme Unisurf, Automatisme,13*, 1968.

[4] C. L. Bottasso, D. Leonello, and B. Savini, "Path planning for autonomous vehicles by trajectory smoothing using motion primitives," *Control Systems Technology, IEEE Transactions on*, vol. 16, no. 6, pp. 1152–1168, 2008.

[5] L. E. Dubins, "On curves of minimal length with a constraint on average curvature, and with prescribed initial and terminal positions and tangents," *American Journal of mathematics*, pp. 497–516, 1957.

[6] M. Hwangbo, J. Kuffner, and T. Kanade, "Efficient two-phase 3d motion planning for small fixed-wing uavs," in *Robotics and Automation, 2007 IEEE International Conference on*. IEEE, 2007, pp. 1035–1041.

[7] V. P. Kostov, E. V. Degtiariova-Kostova *et al.*, "The planar motion with bounded derivative of the curvature and its suboptimal paths," *Acta Math. Univ. Comenianae*, vol. 64, no. 2, pp. 185–226, 1995.

[8] N. Ozalp and O. K. Sahingoz, "Optimal uav path planning in a 3d threat environment by using parallel evolutionary algorithms," in *Unmanned Aircraft Systems (ICUAS), 2013 International Conference on*. IEEE, 2013, pp. 308–317.

[9] M. Shah and N. Aouf, "3d cooperative pythagorean hodograph path planning and obstacle avoidance for multiple uavs," in *Cybernetic Intelligent Systems (CIS), 2010 IEEE 9th International Conference on*. IEEE, 2010, pp. 1–6.

[10] M. Shanmugavel, A. Tsourdos, R. Zbikowski, B. A. White, C. Rabbath, and N. Lechevin, "A solution to simultaneous arrival of multiple uavs using pythagorean hodograph curves," in *American Control Conference, 2006*. IEEE, 2006, p. 6.

[11] T. R. Wan, W. Tang, and H. Chen, "A real-time 3d motion planning and simulation scheme for nonholonomic systems," *Simulation Modelling Practice and Theory*, vol. 19, no. 1, pp. 423–439, 2011.

[12] K. Yang, S. K. Gan, and S. Sukkarieh, "An efficient path planning and control algorithm for ruavs in unknown and cluttered environments," *Journal of Intelligent and Robotic Systems*, vol. 57, no. 1-4, pp. 101–122, 2010.